PAPER

One-pot green synthesis of nanohybrid structures: gold nanoparticles in poly(γ-glutamic acid) copolymer nanoparticles†

Rong-li Zhang,[ab] Sheng Xu,[a] Jing Luo,[a] Dong-jian Shi,[a] Chen Liu[a] and Xiao-ya Liu*[a]

Nanohybrids, comprising gold nanoparticles (Au NPs) and polymer NPs have attracted significant attention in recent years due to their excellent physical and chemical properties. In this work, a novel kind of nanohybrids based on Au NPs and biocompatible poly(γ-glutamic acid)-*graft*-3,4-dihydroxy-L-phenylalanine (γ-PGA-*g*-DA) NPs was conveniently achieved through a green and facile one-pot strategy. By simply adding HAuCl$_4$·3H$_2$O to the aqueous solution of γ-PGA-*g*-DA copolymer, the decrease of the pH value induced the self-assembly of γ-PGA-*g*-DA into NPs, during which Au^{3+} was adsorbed in the *in situ* formed NPs and spontaneously reduced to Au NPs by the dopamine moieties of γ-PGA-*g*-DA, leading to the formation of Au@γ-PGA-*g*-DA nanohybrids. In the reaction process, γ-PGA-*g*-DA was used as scaffold and reductant simultaneously, avoiding the use of extra toxic reducing reagents. Interestingly, the particle size and clustering of Au NPs in Au@γ-PGA-*g*-DA nanohybrids were varied with the loadings of HAuCl$_4$·3H$_2$O. This one-pot preparation process is very simple, fast, and completely based on the principles of green chemistry. Furthermore, the resultant biocompatible Au@γ-PGA-*g*-DA nanohybrids were used to detect L-tryptophan and exhibited a good analytical performance. The novel Au@γ-PGA-*g*-DA nanohybrids are a promising system for detecting the amino acids and biological species.

Introduction

Nanoparticles (NPs) self-assembled from amphiphilic polymers can be useful for many applications, such as drug delivery,[1,2] nanocontainer,[3] catalysts[4] and sensors.[5,6] Au NPs, with attractive size- and shape-related electronic and catalytic properties, have been widely studied in biosensing and biocatalysis.[7] The Au@polymer nanohybrids, incorporating Au NPs into amphiphilic copolymer NPs, combine the unique physical or chemical properties of Au NPs with hierarchical nanophase-separated self-assembly of amphiphilic copolymers[8–14] and are potentially useful in high performance catalysis and sensors.[15–19]

Therefore, considerable efforts have been devoted to synthesizing Au@polymer nanohybrids based on suitable techniques, including the covalent and non-covalent approaches. For example, Xie[20] developed Au@polymer nanohybrids *via* covalent integration of Au NPs with thiol-functionalized, crosslinked and highly branched polymer NPs;

Cuendias[21] used water-dispersible core–shell polyurethane–poly-(acrylic acid) particles to spontaneously reduce Au^{3+} at the particle surface through the thiophene moieties; Chen[22] synthesized Au@polymer nanohybrids *via in situ*-generated Au NPs through the reduction of NaBH$_4$ in triblock copolymer PEG-*b*-PS-*b*-P4VP NPs. Although these approaches can afford well-defined nanohybrids, most of these polymers are not biocompatible or biodegradable. Moreover, none of these methods offer the "green" synthesis. The principles of "green" synthesis include the adoption of less hazardous syntheses; selection of safer starting materials with a good degree of utilization; avoidance of the use of toxic solvents; usage of renewable, biodegradable materials; and minimized energy requirements.[23] With the development of biomedicine and biomaterials, there is a growing requirement to develop environment-friendly processes for Au@polymer nanohybrids production that do not rely on toxic chemicals.

In this study, we offered a facile, simple and "green" synthesis for biocompatible Au@polymer nanohybrids which can be used to detect biological species.

Poly-γ-glutamic acid (γ-PGA) is a biocompatible and biodegradable polymer. Anionic γ-PGA was widely used in food production, cosmetics, agriculture and pharmaceuticals because it is edible and nontoxic to humans and the environment.[24–27] Yu[28] and Stevanović[23] used γ-PGA as stabilizer to synthesize noble metal NPs. They found that the NPs were

[a]Key Laboratory of Food Colloids and Biotechnology, Ministry of Education, School of Chemical and Material Engineering, Jiangnan University, Wuxi 214122, China. E-mail: lxy@jiangnan.edu.cn; Fax: +86-510-85917763; Tel: +86-510-85917763

[b]School of Biochemical Engineering, Anhui Polytechnic University, Wuhu 241000, China. E-mail: zrl326@163.com; Fax: +86-510-85917763; Tel: +86-510-85917763

† Electronic supplementary information (ESI) available. See DOI: 10.1039/c4ra01094a

biocompatible and did not induce a toxicological response of Caco-2 epithelial cells *in vitro*. On the other hand, 3,4-dihydroxy-L-phenylalanine (dopamine, DA) is a neurotransmitter which has low oxidation potential, excellent surface adhesion properties, hydrophobic benzene ring and good biocompatibility.[29–32] The *in situ* reduction of Au^{3+} anions to Au NPs *via* dopamine and polydopamine has been reported in previous articles.[33,34]

Here, γ-PGA and dopamine were used as hydrophilic backbone and hydrophobic side chain respectively to synthesize a biocompatible poly(γ-glutamic acid)-*graft*-3,4-dihydroxy-L-phenylalanine (γ-PGA-*g*-DA) copolymer. The resultant γ-PGA-*g*-DA copolymer was in dissolution state in neutral aqueous solution and could self-assemble into NPs at low pH. When $HAuCl_4 \cdot 3H_2O$ was added to the γ-PGA-*g*-DA copolymer solution, the decrease of the pH value induced the self-assembly of γ-PGA-*g*-DA into NPs, during which Au^{3+} was adsorbed in the *in situ* formed NPs *via* the adhesion interaction of dopamine and the electrostatic interaction between Au^{3+} and COO^- group. The self-assembly of γ-PGA-*g*-DA accompanied by spontaneous reduction of Au^{3+} through dopamine moieties of γ-PGA-*g*-DA led to the formation of Au@γ-PGA-*g*-DA nanohybrids. The schematic illustration for the formation of Au@γ-PGA-*g*-DA nanohybrids is shown in Fig. 1. In the process of fabricating biocompatible Au@γ-PGA-*g*-DA nanohybrids, γ-PGA-*g*-DA was used as the scaffold and reductant simultaneously, avoiding the use of extra toxic reducing reagents. This is a facile, quick, green preparation procedure for synthesis of biocompatible nanohybrids. The obtained Au@γ-PGA-*g*-DA nanohybrids have potential application for detecting the biology species and biomedical imaging.

Experimental section

Materials

γ-PGA (sodium salt, M_w 700 000–100 000 kDa) was purchased from AMRESCO, USA. 1-(3-Dimethylaminopropyl)-3-ethyl-carbodiimide hydrochloride (EDC·HCl), N-hydroxysuccinimide (NHS), 3,4-dihydroxy-L-phenylalanine (dopamine, DA), hydrochloric acid (HCl), hydrogen tetrachloroaurate trihydrate (HAuCl$_4$·3H$_2$O), sodium chloride (NaCl), sodium hydroxide (NaOH), phosphate, L-lysine, L-phenylalanine, L-histidine, L-glycine, L-alanine, L-proline and L-tryptophan were supplied by Aladdin.

Synthesis of γ-PGA-*g*-DA

2 mmol γ-PGA was dissolved in 40 mL deionized water under stirring in an ice-bath. After 0.5 h, 2 mmol EDC·HCl and 4 mmol of NHS were added into the resulted solution. After 5 min of stirring, 2 mmol dopamine was added to the mixture and the reaction was carried out in an ice-bath for another hour and then at room temperature overnight. The γ-PGA-*g*-DA copolymer was purified *via* dialysis using a dialysis membrane (MC: 14 000) in deionized water. Purification was considered to be complete when no free dopamine was detectable in the wash solution by UV. Finally, the washed γ-PGA-*g*-DA copolymer solution was frozen and then lyophilized.

Self-assembly of γ-PGA-*g*-DA copolymer

The γ-PGA-*g*-DA copolymer, which contains $-COO^-$ and dopamine moieties at the side chains, is an anionic polyelectrolyte with pH-responsiveness. After the copolymer was dissolved in deionized water, aqueous HCl was used to adjust the pH value of the solution. With decreasing the pH value of copolymer solution, the copolymer self-assembled and aggregated into NPs. A volume of 10 mL of the γ-PGA-*g*-DA copolymer solution was removed at different pH values and left for 24 h to equilibrate before the measurements.

Fabrication of the Au@γ-PGA-*g*-DA nanohybrids

The Au@γ-PGA-*g*-DA nanohybrid was synthesized using a chemical reduction method wherein γ-PGA-*g*-DA NPs served as a reduction reagent and a scaffold. A stock solution of 0.2 mg mL^{-1} γ-PGA-*g*-DA was prepared in deionized water. An aliquot of a 0.1 mg mL^{-1} HAuCl$_4$·3H$_2$O solution was added to the γ-PGA-*g*-DA stock solution with vigorous stirring.[35] The molar ratio of Au^{3+} to the repeated units of γ-PGA-*g*-DA (L_{Au}) was 0.30, 0.15 and 0.10, respectively. The Au^{3+} ions were bound to the catechol group of the dopamine and $-COO^-$ of γ-PGA-*g*-DA copolymer. The pH value of the mixture decreased to 3.60 with the addition of an aqueous solution of HAuCl$_4$, resulting in the formation of γ-PGA-*g*-DA NPs. The Au NPs were then formed *via* the spontaneous reduction of Au^{3+} through the catechol groups of γ-PGA-*g*-DA at room temperature in the dark.

Detection of Au@γ-PGA-*g*-DA nanohybrids for L-tryptophan

Au NPs have been used to modify electrode to determine biological species due to their good biocompatibility, electrochemistry and catalytic properties.[36–38] The Au@γ-PGA-*g*-DA nanohybrids, which combine the advantages of the Au NPs and γ-PGA-*g*-DA NPs, can be used to modify electrode to detect biological species. Prior to the modification, a bare glassy carbon electrode (GCE) was polished by polishing cloth having alumina particles and cleaned by ultra-sonication in ethanol, acetone and ultrapure water. After 10 μL Au@γ-PGA-*g*-DA

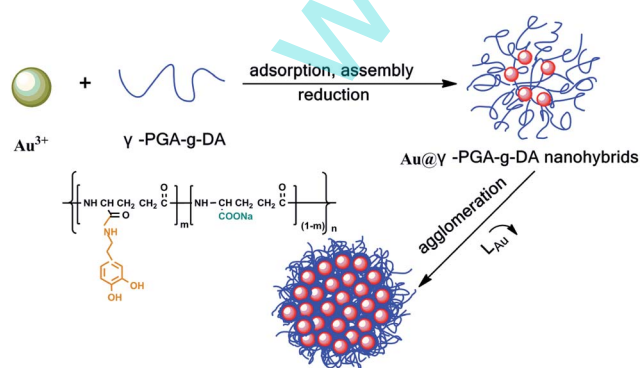Fig. 1 Schematic illustration for the formation of Au@γ-PGA-*g*-DA nanohybrids. L_{Au} is the molar ratio of Au^{3+} to the repeated units of γ-PGA-*g*-DA.

nanohybrids solution was cast on the GCE, a beaker was used to cover the electrode to enable the slow evaporation of water in air. Then the Au@γ-PGA-g-DA/GCE was obtained and stored at 4 °C in a refrigerator before use.

Characterization

^{1}H NMR spectrum was recorded using a Bruker (400 MHz) instrument. Approximately 50 mg of copolymer was dissolved in 500 μL of D_2O and analyzed with a Bruker instrument with a ^{1}H NMR measuring program. Infrared (IR) experiment was run by attenuate total reflexion (ATR) mode on a Nicolet FI-IR Spectrometer instrument. IR spectra were collected in the wavelength range of 4000 to 500 cm^{-1}. UV-Vis spectra were recorded on a TU-1901 spectrophotometer. Solution pH value was monitored using a pHS-3C precision digital pH meter. Dynamic light scattering (DLS) experiment was conducted using an ALV-5000/E dynamic light scattering instrument at 90°. All polymer solutions (0.1 mg mL^{-1}) were passed through 0.8 μm Millipore filters prior to loading into the sample cell. X-ray photoelectron spectroscopy (XPS) measurement was made on a VG ESCALAB MkII spectrometer with a Mg Ka X-ray source (1253.6 eV photos). The X-ray source was operated at 14 kV and 20 mA. X-ray diffraction (XRD) profiles of Cu-modified graphene were obtained (XD-3A, Shimadzu) with high-intensity Cu Kα radiation ($\lambda = 1.5406$ nm). Thermal gravimetric analysis (TGA) was conducted on an SDT 2960 instrument from room temperature to 800 °C with a heating rate of 2°C min^{-1} in the nitrogen flow (10 mL min^{-1}). Transmission electron microscopy (TEM) image was recorded in a JEOL JEM-2100 at 200 kV. A drop of a 0.1 mg mL^{-1} aqueous solution (approximately 7 μL) was cast onto a carbon-coated copper grid. The sample was then allowed to dry under ambient conditions. The morphology of the nanohybrids was observed using a Hitachi S-4800 field emission scanning electron microscope (FESEM) operating at 5 kV. Atomic force microscope (AFM) was performed on a CSPM3300 (Benyuan Co.) with a vertical resolution of 0.1 nm and a horizontal resolution of 0.2 nm. Electrochemical experiment was performed on an Epsilon electrochemical workstation (BAS, USA) using a three electrode system. The modified electrode was used as the working electrode. A saturated calomel electrode (SCE, Aida, Tianjin, China) and a platinum electrode (Aida, Tianjin, China) served as the reference and counter electrodes, respectively. The potentials applied to the working electrode were in reference to the SCE.

Results and discussion

Characterization of γ-PGA-g-DA copolymer

The structure of γ-PGA-g-DA was determined by ^{1}H NMR. As can be seen in Fig. S1 in ESI,† compared with γ-PGA, new aromatic ring (6.4–7.0 ppm) peaks appeared in the ^{1}H NMR spectrum of the γ-PGA-g-DA copolymer (Fig. S1B†), indicating that dopamine has been successfully introduced into γ-PGA side chain. The grafting degree of γ-PGA-g-DA copolymer was determined by ^{1}H NMR using integrals of the α-H of γ-PGA skeleton and the benzyl-CH_2 overlapped signals of dopamine. The unlabeled

chemical shift values were attributed to the intermediate form of γ-PGA that resulted from the catalysis of EDC and NHS.[39] The FT-IR spectra of γ-PGA and γ-PGA-g-DA are shown in Fig. S2.† The peaks at 1570 cm^{-1} and 1392 cm^{-1} for γ-PGA showed the asymmetric and symmetric stretching vibration modes of –COO$^-$ which were reduced in γ-PGA-g-DA, indicating successful synthesis of γ-PGA-g-DA copolymer.

Self-assembly of γ-PGA-g-DA copolymer

The self-assembly behavior of the amphiphilic copolymer was usually monitored through the turbidity experiment.[40] The turbidities of 0.1 mg mL^{-1} aqueous solutions of γ-PGA and γ-PGA-g-DA copolymer at 550 nm as a function of solution pH are shown in Fig. S3.† As can be seen, the turbidities of γ-PGA aqueous solution showed negligible change from pH 5.50 to pH 2.00, indicating that no NPs were formed in the pH range of 5.50–2.00. In contrast, the turbidities of γ-PGA-g-DA-20 and γ-PGA-g-DA-28 exhibited a clear break point at pH 3.20 and pH 3.50, respectively, indicating the formation of NPs at low pH value. The possible reason is that with the decrease of pH value, the protonation of the hydrophilic carboxyl group makes γ-PGA-g-DA more hydrophobic, leading to self-assembly of the copolymer and formation of the NPs. In addition, the pH value at which the γ-PGA-g-DA NPs formed decreased with the decreasing the grafting degree γ-PGA-g-DA copolymer due to the decrease of hydrophobicity of copolymer. As pH value further decreased, the turbidities sharply increased. The significant increasing turbidity may be ascribed to the small NPs agglomerating to large particles, as a result of the weakening electrostatic repulsion between the NPs with further decreasing pH value. Below pH 3.00, macroscopic precipitation was observed.

The self-assembly of γ-PGA-g-DA-28 copolymer was also investigated by DLS and TEM measurements. As shown in Fig. 2, the copolymer had an average hydrodynamic diameter of 248.2 nm at pH 4.50. However, the TEM image shows the uniformly spherical morphology with a size of 36 nm (obtained by analysis with *Nanomeasurer* software). The reason may be ascribed to the folding of the coil-like γ-PGA-g-DA copolymer in aqueous solution after the evaporation of water. When pH was decreased to pH 3.50, the average hydrodynamic diameter of γ-PGA-g-DA copolymer was 99.6 nm and the TEM image revealed a spherical morphology with an average diameter of 103 nm, indicating that the γ-PGA-g-DA NPs were formed and had compact structure at pH 3.50 in aqueous solution. When the pH value further decreased to pH 3.10, the DLS revealed that the γ-PGA-g-DA NPs became larger with an average hydrodynamic diameter of 270.4 nm, which was confirmed by TEM measurement. The possible reason is that the further protonation of the carboxyl groups and the decrease of the negative charge led to the agglomeration of NPs.

In addition, the self-assembly of γ-PGA-g-DA-28 aqueous solutions and the size of copolymer NPs with the concentration from 0.05 mg mL^{-1} to 2 mg mL^{-1} were investigated by turbidity and DLS experiments. As can be seen in Fig. S4,† γ-PGA-g-DA-28 formed NPs between pH 3.10 and pH 4.00 varying with concentration. With increasing the concentration, the pH value
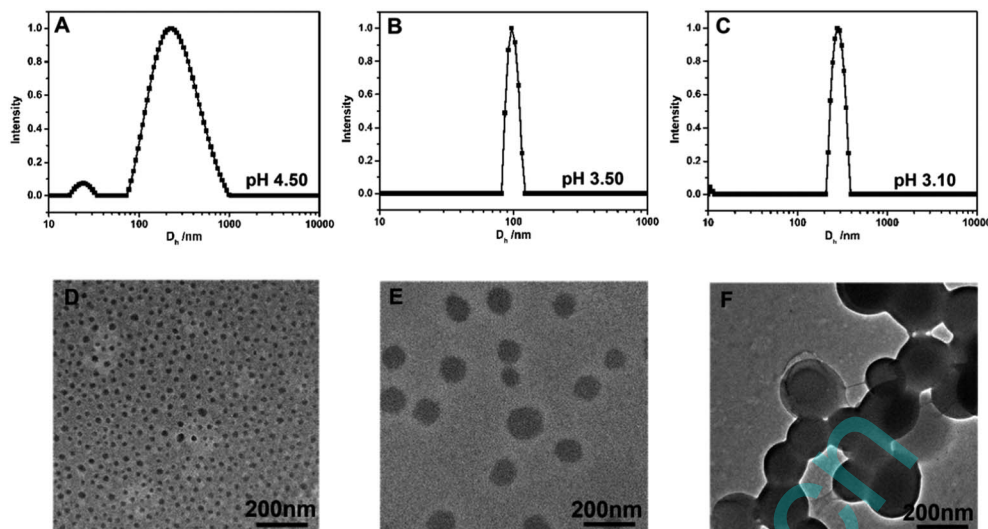
Fig. 2 Size distribution of the γ-PGA-g-DA in an aqueous solution of pH 4.50, 3.50 and 3.10 (A–C) and the corresponding TEM images (D–F).

at which the NPs formed increased. When the concentration of γ-PGA-g-DA aqueous solution was above 2 mg mL^{-1}, macroscopic precipitation was observed. The relationship of the pH value at which the NPs formed and the concentration were shown in Fig. S4 (B).† The γ-PGA-g-DA aqueous solution of 0.1 mg mL^{-1} which formed the γ-PGA-g-DA NPs with minimum size was chosen to prepare Au@γ-PGA-g-DA nanohybrids.

Preparation of Au@γ-PGA-g-DA nanohybrids

After the self-assembly of γ-PGA-g-DA copolymer have been investigated, we turn to study the synthesis of Au@γ-PGA-g-DA nanohybrids. The HAuCl$_4$ aqueous solution was added by dropwise into the γ-PGA-g-DA copolymer aqueous solution while stirring, leading to the simultaneous self-assembly of the copolymer and the reduction of Au^{3+}. The characteristic colors of the Au@γ-PGA-g-DA nanohybrids depending on the L_{Au} are shown in Fig. 3 (inset).

The UV-Vis absorption spectra were recorded for Au@γ-PGA-g-DA nanohybrids with different L_{Au} (Fig. 3). All samples

Fig. 3 UV-Vis absorption spectra and the characteristic colors (inset) for Au@γ-PGA-g-DA nanohybrids with different L_{Au}. L_{Au} is the molar ratio of Au^{3+} to the repeated units of γ-PGA-g-DA.

exhibited an absorption maximum near a wavelength (λ_{max}) of 550 nm, which corresponds to the surface plasmon absorption of Au,[41] confirming the presence of Au NPs. As L_{Au} decreased from 0.30 to 0.15, the λ_{max} values were red-shifted from 518 to 533 nm. When L_{Au} reached 0.10, the absorption peak became much broader and λ_{max} shifted to about 580 nm. Besides the increase of particle size, the agglomeration of smaller particles is another reason for the red shift of λ_{max} values with decreasing L_{Au}.[38,42] For the Au@γ-PGA-g-DA nanohybrids with L_{Au} 0.30, L_{Au} 0.15 and L_{Au} 0.10, the solutions remained clear without precipitation, even for several months. However, for the Au@γ-PGA-g-DA nanohybrids with $L_{Au} > 0.30$, the solution became turbid upon addition of HAuCl$_4$, and precipitation of darkly colored solids was observed during redox reaction. The possible reason is that for higher L_{Au}, much more Au NPs were reduced by the dopamine groups, while the γ-PGA-g-DA NPs were unable to stabilize so much Au NPs, leading to the precipitation of Au@γ-PGA-g-DA nanohybrids.

The particle size and clustering of Au NPs were determined by TEM measurement (Fig. 4). At the highest values of L_{Au} studied (0.30), TEM image revealed that the Au NPs had a spherical shape and a uniform distribution. The γ-PGA-g-DA NPs, which were not observed due to the lower density, provided a scaffold for Au NPs and prevented the aggregation of the in situ reduced Au. The average size of Au NPs determined by TEM was 5.0 nm with sizes ranging from 1.8–8.1 nm via analysis with Nanomeasurer software. When L_{Au} decreased to 0.15, the size of the Au NPs increased to approximately 20 nm; and groups of large particles with some clustering were observed instead of small particles. The trend in particle size with decreasing L_{Au} has been reported for other reduction/stabilizer systems.[43,44] The formation of large, irregular and agglomerated particles at lower loading ratios might be encouraged by the clustering of unreacted dopamine groups and metal particles.[38] For the Au@γ-PGA-g-DA nanohybrids with L_{Au} 0.10, the small particles disappeared, and groups of large irregular particles were

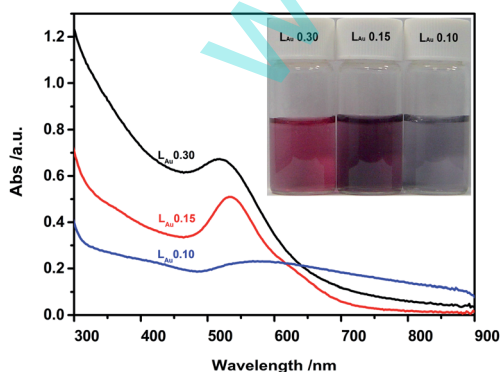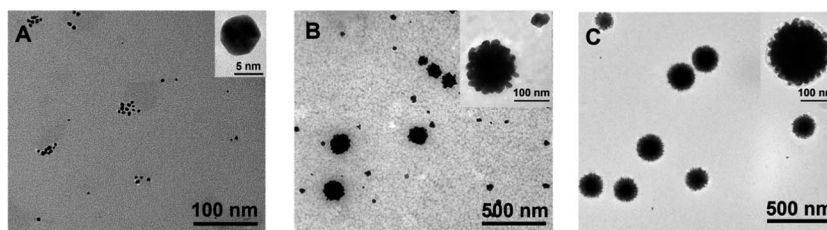Fig. 4   TEM images for Au@γ-PGA-g-DA nanohybrids with different L_{Au}; L_{Au} is the molar ratio of Au^{3+} to the repeated units of γ-PGA-g-DA. (A) L_{Au} 0.30, (B) L_{Au} 0.15 and (C) L_{Au} 0.10.

observed instead. In addition, the copolymer shell of the large irregular particle also can be clearly observed. The possible reason is that with increasing the copolymer, the interaction of unreacted dopamine groups and Au NPs and the entanglement of copolymer led to the collapse of copolymer shell on the Au NPs surface, which decreases shell thickness and increases the internal polymer density of the shell.

In addition, the unmodified γ-PGA, dopamine, mixture of γ-PGA and dopamine, and γ-PGA-g-DA-20 copolymer with L_{Au} 0.30 were used to prepare nanohybrids respectively. The UV-vis spectra and TEM images were shown in Fig. S5 and S6, respectively.†

As can be seen in Fig. S5,† UV-vis spectra of the nanohybrids prepared from unmodified γ-PGA, DA alone or γ-PGA mixed with DA exhibited a very broad absorption from 490 nm to 750 nm, indicating the agglomeration of the Au NPs, which were confirmed by the TEM measurements. However, the UV-vis spectra of the nanohybrids prepared from γ-PGA-g-DA-28 copolymer with L_{Au} 0.30 exhibited a narrow absorption with absorption maximum wavelength of 513 nm, which corresponds to the surface plasmon absorption of Au NPs. The TEM image revealed that the Au NPs had a spherical shape and a uniform distribution in nanohybrids. The agglomeration of the Au NPs prepared from the unmodified γ-PGA, DA alone or γ-PGA mixed with DA can be ascribed to clustering of metal particles and dopamine or γ-PGA. The unmodified γ-PGA, DA alone or γ-PGA mixed with DA was ineffective to isolate the Au NPs during the process of in suit reduction due to their molecule state in aqueous. In contrast, by simply adding HAuCl$_4$·3H$_2$O to the aqueous solution of γ-PGA-g-DA-28 copolymer, the decrease of the pH value induced the self-assembly of γ-PGA-g-DA into NPs, during which Au^{3+} was adsorbed and immobilized via dopamine and COO$^-$ groups in the in situ formed NPs and spontaneously reduced to Au NPs by the dopamine moieties of γ-PGA-g-DA, leading to the formation of small, well-dispersed Au NPs in nanohybrids. The results of control experiment revealed that the in situ formed γ-PGA-g-DA NPs severed as a scaffold for Au NPs and effective to isolate the Au NPs during the process of in suit reduction.

The UV-Vis spectra and TEM images of Au@γ-PGA-g-DA prepared from different grafting degree were shown in Fig. S5 and S6, respectively.† As can be seen in Fig. S5,† compared with the nanohybrids prepared from γ-PGA-g-DA-28 copolymer with L_{Au} 0.30, the λ_{max} values of the nanohybrids prepared from γ-PGA-g-DA-20 copolymer with L_{Au} 0.30 were red-shifted from

513 to 529 nm, indicating the size increase of Au NPs in the nanohybrids prepared from γ-PGA-g-DA-20 copolymer. The TEM measurement confirmed the size increase of Au NPs in the nanohybrids prepared from γ-PGA-g-DA-20 copolymer. The possible reason is that with the same L_{Au}, the ratio of the stabilizer to the reductant was increased in the γ-PGA-g-DA-20 copolymer compared with the γ-PGA-g-DA-28 copolymer; the increase of stabilizer and the decrease of reductant decreased the reduction rate of Au NPs, leading to the agglomeration and size increase of Au NPs in the nanohybrids. The nanohybrids prepared from γ-PGA-g-DA-28 copolymer with L_{Au} 0.30 exhibited smaller, well-dispersed Au NPs in nanohybrids.

The crystallinity of the Au NPs in Au@γ-PGA-g-DA nanohybrids was investigated by XRD. Fig. S7(A) shows the XRD patterns for the Au@γ-PGA-g-DA nanohybrids and γ-PGA-g-DA bulk powder.† Compared with the diffractogram of γ-PGA-g-DA bulk powder, the diffractogram of Au@γ-PGA-g-DA nanohybrids shows five additional characteristic reflections around at 38°, 44°, 64°, 78°, and 82° in addition to one broad diffraction peak between 20° and 30° originating from γ-PGA-g-DA copolymer, corresponding to the (111), (200), (220), (311) and (222) of the lattice plane of gold respectively, indicating the presence of Au NPs in the Au@γ-PGA-g-DA nanohybrids.[45,46]

In order to further investigate the composition of the Au@γ-PGA-g-DA nanohybrids, Au@γ-PGA-g-DA nanohybrids and γ-PGA-g-DA bulk powder were analyzed by XPS. Fig. S7(B) represents the XPS surveys of Au@γ-PGA-g-DA nanohybrids and γ-PGA-g-DA bulk powder.† The presence of peaks due to Au4f in survey spectra of Au@γ-PGA-g-DA nanohybrids in addition to the three main peaks originating from O1s, C1s and N1s confirms the presence of Au in the nanohybrid materials.[47] Such peaks are not present in survey spectra of γ-PGA-g-DA bulk powder.

To explain and for better understand the mechanism of the interactions between the γ-PGA-g-DA copolymer and Au NPs, FT-IR were performed to study the type of chemical bonds involved in the interactions between the γ-PGA-g-DA copolymer with Au NPs. As shown in Fig. S7(C),† the peaks of carboxylate group at 1390 cm^{-1} and the amide groups at 2930 and 1526 cm^{-1} decreased in the FT-IR spectrum of Au@γ-PGA-g-DA nanohybrids compared with the FT-IR spectrum of γ-PGA-g-DA copolymer, implying the chemical bonds involved in the interactions between the Au NPs and either the carboxylate groups or the amide groups.[45,46]

TGA of the Au@γ-PGA-g-DA nanohybrids and γ-PGA-g-DA bulk powder was performed in order to find their thermal

stability and also to evaluate their composition.[47] The TGA traces of them are shown in Fig. S7(D).† In all the samples, the first loss in weight started at 100 °C probably due to the decrease of water in weight. The second loss in weight was probably due to the degradation of γ-PGA-g-DA chain started at 168 °C for γ-PGA-g-DA bulk powder while it began at 146 °C for Au@γ-PGA-g-DA nanohybrids. The amount of Au was found to be 6.8% in nanohybrids estimated by TGA traces.

The size distribution of Au@γ-PGA-g-DA nanohybrids with L_{Au} 0.30 in aqueous solution were investigated by DLS measurement. As can be seen in Fig. S8(A),† the average hydrodynamic diameter of the Au@γ-PGA-g-DA nanohybrids with L_{Au} 0.30 was found to be approximately 187 nm in the aqueous solution, implying that the Au NPs were entrapped and stabilized by the γ-PGA-g-DA NPs. The morphology of nanohybrids in dry state was investigated by SEM and AFM. As shown in Fig. S8(B–D),† various morphologies (including sphere and polygon) were observed. The possible reason is that the nanohybrids were easy to deform during the drying process due to they were in swelling state in aqueous solution.

The stability of Au@γ-PGA-g-DA nanohybrids was investigated in different pH buffers and salines using UV-Vis and DLS measurements.[48] As shown in Fig. S9,† with increasing the pH values and salines, the average size of nanohybrids slightly increased resulted from the deprotonation of γ-PGA-g-DA copolymer. In addition, UV-Vis spectra with different pH buffers and salines revealed no shift in the localized surface plasmon resonance (LSPR) band of the Au@γ-PGA-g-DA nanohybrids, implying that no aggregation occurred and the nanohybrids exhibit high colloidal stability.

Detection of Au@γ-PGA-g-DA nanohybrids for L-tryptophan

The film formed from Au@γ-PGA-g-DA nanohybrids was investigated by SEM and AFM (Fig. S10†). As can be seen, plenty of Au NPs appeared on the Au@γ-PGA-g-DA nanohybrids film of electrode surface.

The electrochemical response of Au@γ-PGA-g-DA nanohybrids for L-tryptophan were performed in 0.1 mol L^{-1} phosphate buffer solution (PBS 7.0). Fig. 5A shows the DPSV

curves obtained in various concentrations of L-tryptophan. The peaks appeared at 0.6–0.7 V is assigned to the characteristic oxidation peak of L-tryptophan in phosphate buffer solution.[49,50] With increasing the concentration of L-tryptophan, the oxidation peak current of L-tryptophan increased, indicating that the Au@γ-PGA-g-DA nanohybrids showed good detection performance for L-tryptophan. The linear dynamic ranges as shown in Fig. 5B from 1×10^{-6} to 8×10^{-4} mol L^{-1}, with a correlation coefficient of 0.997. The linear regression equations is as follows: I_p (μA) = 30.52 + 4.48lgC$_{L\text{-tryptophan}}$(mol L^{-1}).

The influences of some amino acids (L-lysine, L-serine, L-phenylalanine, L-histidine, L-glycine, L-alanine, and L-proline) were tested by analyzing a standard solution of 1×10^{-5} mol L^{-1} L-tryptophan via the Au@γ-PGA-g-DA nanohybrids.[51] As shown in Fig. S11,† the mixture of L-tryptophan and 50-fold concentrations amino acids of aforementioned interfering substances caused a change in the signal of below 5%, indicating that the Au@γ-PGA-g-DA nanohybrids showed good selectivity for L-tryptophan.

To demonstrate the performance of Au@γ-PGA-g-DA nanohybrids in real sample analysis, the determination of L-tryptophan in human blood samples were analyzed at the Au@γ-PGA-g-DA-modified GCE. The human blood serum samples were diluted to 100 times with 0.1 mol L^{-1} phosphate buffer solution (pH 7.0) without any treatment. Then, the Au@γ-PGA-g-DA-modified GCE was applied to detect human blood serum samples spiked with L-tryptophan at a certain concentration.[51] The results were listed in Table 1. The recoveries of the method are satisfactory and in the range of 98–105%, indicating that Au@γ-PGA-g-DA nanohybrids are a promising system for detecting the amino acids.

Table 1 Determination of L-tryptophan in blood samples

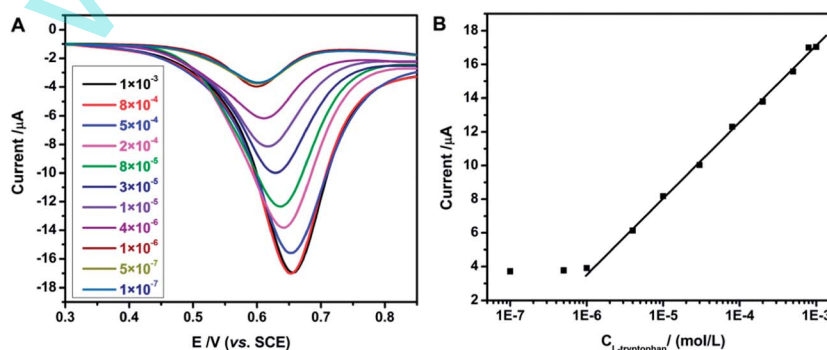| Blood sample	Added (mol L^{-1})	Found (mol L^{-1})	Recovery (%)
Sample 1	5×10^{-5}	4.91×10^{-5}	98.2
Sample 2	1×10^{-5}	1.03×10^{-5}	103
Sample 3	5×10^{-4}	4.95×10^{-4}	99

Fig. 5 DPSV curves of Au@γ-PGA-g-DA-modified GCE in 0.1 mol L^{-1} phosphate buffer solution (PBS 7.0) containing different concentrations of L-tryptophan from 1×10^{-7} mol L^{-1} to 1×10^{-3} mol L^{-1} (A) and the corresponding calibration curve of L-tryptophan with different concentrations (B).

Conclusions

We reported a new approach for the green synthesis of biocompatible Au@γ-PGA-g-DA nanohybrids. In a typical synthesis, an aqueous metal precursor solution was added to γ-PGA-g-DA solution wherein γ-PGA-g-DA served as both effective reductant and scaffold. The results revealed that L_{Au} is clearly a key parameter governing the size and degree of clustering of the Au NPs in fabrication of Au@γ-PGA-g-DA nanohybrids. The optimal composition for preparation of small, well-dispersed Au NPs in nanohybrids is L_{Au} 0.30. The obtained Au@γ-PGA-g-DA nanohybrids have great promise in biological fields due to their green synthesis, simple preparation procedure, water-dispersibility and biocompatibility.

Acknowledgements

References

1 C. Wei, J. Guo and C. Wang, *Macromol. Rapid Commun.*, 2011, **32**, 451–455.

2 A. Blanazs, S. P. Armes and A. J. Ryan, *Macromol. Rapid Commun.*, 2009, **30**, 267–277.

3 Y. P. Wang, P. Han, H. P. Xu, Z. Q. Wang, X. Zhang and A. V. Kabanov, *Langmuir*, 2010, **26**, 709–715.

4 Z. S. Ge, D. Xie, D. Y. Chen, X. Z. Jiang, Y. F. Zhang, H. W. Liu and S. Y. Liu, *Macromolecules*, 2007, **40**, 3538–3546.

5 Y. Q. Yang, C. L. Yi, J. Luo, R. Liu, J. C. Liu, J. Q. Jiang and X. Y. Liu, *Biosens. Bioelectron.*, 2011, **26**, 2607–2612.

6 Z. Li, J. F. Ding, M. Day and Y. Tao, *Macromolecules*, 2006, **39**, 2629–2636.

7 M. H. Lin, H. Pei, F. Yang, C. H. Fan and X. L. Zuo, *Adv. Mater.*, 2013, **25**, 3490–3496.

8 R. Shenhar and V. M. Rotello, *Acc. Chem. Res.*, 2003, **36**, 549–561.

9 M. C. Daniel and D. Astruc, *Chem. Rev.*, 2004, **104**, 293–346.

10 C. S. Cho, W. Choi, P. H. C. Camargo and Y. Xia, *Langmuir*, 2010, **26**, 10005–10012.

11 M. Adeli, R. S. Sarabi, R. Y. Farsi, M. Mahmoudi and M. Kalantari, *J. Mater. Chem.*, 2011, **21**, 18686–18695.

12 J. Y. Mao, X. X. Qi, X. Q. Cao, J. M. Lu, Q. F. Xu and H. W. Gu, *Chem. Commun.*, 2011, **47**, 4228–4230.

13 W. Han, M. Byun, B. Li, X. C. Pang and Z. Q. Lin, *Angew. Chem.*, 2012, **124**, 12756–12760.

14 T. L. Rao, X. H. Dong, B. C. Katzenmeyer, C. Wesdemiotis, S. Z. D. Cheng and M. L. Becker, *Soft Matter*, 2012, **8**, 2965–2971.

15 M. R. Bockstaller and E. L. Thomas, *J. Phys. Chem. B*, 2003, **107**, 10017–10024.

16 J. Y. Cheng, C. A. Ross, V. Z. H. Chan, E. L. Thomas, R. G. H. Lammertink and G. Vancso, *J. Adv. Mater.*, 2001, **13**, 1174–1178.

17 T. F. Jaramillo, S. H. Baeck, B. R. Cuenya and E. W. McFarland, *J. Am. Chem. Soc.*, 2003, **125**, 7148–7149.

18 S. C. Mui, P. E. Trapa, B. Huang, P. P. Soo, M. I. Lozow, T. C. Wang, R. E. Cohen, A. N. Mansour, S. Mukerjee, A. M. Mayes and D. R. Sadoway, *J. Electrochem. Soc.*, 2002, **149**, A1610–A1615.

19 S. G. Jang, A. Khan, M. D. Dimitriou, B. J. Kim, N. A. Lynd, E. J. Kramer and C. J. Hawker, *Soft Matter*, 2011, **7**, 6255–6263.

20 M. Xie, L. Ding, Z. W. You, D. Y. Gao, G. D. Yang and H. J. Han, *J. Mater. Chem.*, 2012, **22**, 14108–14118.

21 A. Cuendias, R. Backov, E. Cloutet and H. Cramail, *J. Mater. Chem.*, 2005, **15**, 4196–4199.

22 X. Chen, Y. L. An, D. Y. Zhao, Z. P. He, Y. Zhang, J. Cheng and L. Q. Shi, *Langmuir*, 2008, **24**, 8198–8204.

23 M. Stevanović, I. Savanović, V. Uskoković, S. D. Škapin, I. Bračko, U. Jovanović and D. Uskokovi, *Colloid Polym. Sci.*, 2012, **290**, 221–231.

24 T. Sekine, T. Nakamura, Y. Shimizu, H. Ueda, K. Matsumoto, Y. Takimoto and T. Kiyotani, *J. Biomed. Mater. Res.*, 2000, **35**, 305–310.

25 M. Kadowaki and T. Noguchi, *Biosci., Biotechnol., Biochem.*, 2001, **65**, 516–521.

26 F. Shi, Z. Xu and P. Cen, *Biotechnol. Bioprocess Eng.*, 2006, **11**, 251–257.

27 X. Y. Yong, W. Raza, G. H. Yu, W. Ran, Q. R. Shen and X. M. Yang, *Bioresour. Technol.*, 2011, **102**, 7548–7554.

28 D. G. Yu, *Colloids Surf., B*, 2007, **59**, 171–178.

29 H. Lee, S. M. Dellatore, W. M. Miller and P. B. Messersmith, *Science*, 2007, **318**, 426–430.

30 M. D. Shultz, J. U. Reveles, S. N. Khanna and E. E. Carpenter, *J. Am. Chem. Soc.*, 2007, **129**, 2482–2487.

31 T. Shalev, A. Gopin, M. Bauer, R. W. Stark and S. Rahimipour, *J. Mater. Chem.*, 2012, **22**, 2026–2032.

32 J. H. Jiang, L. P. Zhu, L. J. Zhu, B. K. Zhu and Y. Y. Xu, *Langmuir*, 2011, **27**, 14180–14187.

33 L. Q. Guo, Q. Liu, G. l. Li, J. B. Shi, J. Y. Liu, T. Wang and G. B. Jiang, *Nanoscale*, 2012, **4**, 5864–5867.

34 Y. H. Zhu, D. Q. Wang, L. Zhang, F. Sun, J. Q. Xu, S. Y. Jiang and Q. M. Yu, *RSC Adv.*, 2013, **3**, 10154–10157.

35 H. P. Chen, D. M. Lentz and R. C. Hedden, *J Nanopart Res.*, 2012, **14**, 690–705.

36 R. N. Goyal, S. Bishnoi, H. Chasta, M. Aziz and M. Oyama, *Talanta*, 2011, **85**, 2626–2631.

37 Y. J. Guo, S. J. Guo, Y. X. Fang and S. J. Dong, *Electrochim. Acta*, 2010, **55**, 3927–3931.

38 H. H. Liu, Y. L. Chen, Y. C. Liu and Z. S. Yang, *J. Solid State Electrochem.*, 2013, **17**, 2623–2631.

39 C. Wang, Q. Yan, H. B. Liu, X. H. Zhou and S. J. Xiao, *Langmuir*, 2011, **27**, 12058–12068.

40 J. Xu, H. Y. Bai, C. L. Yi, J. Luo, C. Yang, W. S. Xia and X. Y. Liu, *Carbohydr. Polym.*, 2011, **86**, 678–683.

41 P. Mulvaney, *Langmuir*, 1996, **12**, 788–800.

42 D. G. Yu, W. C. Lin, C. H. Lin, L. M. Chang and M. C. Yang, *Mater. Chem. Phys.*, 2007, **101**, 93–98.

43 D. V. Leff, P. C. Ohara, J. R. Heath and W. M. Gelbart, *J. Phys. Chem.*, 1995, **99**, 7036–7041.

44 M. J. Hostetler, J. E. Wingate, C. J. Zhong, J. E. Harris, R. W. Vachet, M. R. Clark, J. D. Londono, S. J. Green, J. J. Stokes, G. D. Wignall, G. L. Glish, M. D. Porter, N. D. Evans and R. W. Murray, *Langmuir*, 1998, **14**, 17–30.

45 S. Sekowski, N. Cheval, O. Liszka, V. Astachov, C. Fowkes and A. Fahmi, *Colloids Surf., A*, 2013, **417**, 170–178.

46 M. Adeli, R. S. Sarabi, R. Y. Farsi, M. Mahmoudib and M. Kalantari, *J. Mater. Chem.*, 2011, **21**, 18686–18695.

47 M. Mumtaz, E. Cloutet, C. Labrugère, G. Hadziioannou and H. Cramail, *Polym. Chem.*, 2013, **4**, 615–622.

48 M. S. Strozyk, M. Chanana, I. Pastoriza-Santos, J. Pérez-Juste and L. M. Liz-Marzán, *Adv. Funct. Mater.*, 2012, **22**, 1436–1444.

49 O. J. D'Souza, R. J. Mascarenhas, T. Thomas, I. N. N. Namboothiri, M. Rajamathi, P. Martis and J. Dalhalle, *J. Electroanal. Chem.*, 2013, **704**, 220–226.

50 T. Thomas, R. J. Mascarenhas, O. J. D'Souza, P. Martis, J. Dalhalle and B. E. K. Swamy, *J. Colloid Interface Sci.*, 2013, **402**, 223–229.

51 S. Y. Zhu, J. Zhang, X. E. Zhao, H. Wang, G. B. Xu and J. M. You, *Microchim. Acta*, 2014, **181**, 445–451.